Acta Geologica Polonica, Vol. 76 (2026), No. 2, e85
DOI: 10.24425/agp.2026.158199

Integrating initial shear modulus (G_0) derived from seismic data with long-term deep-seated inclinometer displacements at selected Polish Outer Carpathian flysch landslides

KAMIL WASILEWSKI[1,2], RADOSŁAW MIESZKOWSKI[1], STANISŁAW MIESZKOWSKI[1], and TOMASZ GODLEWSKI[3]

[1] *Faculty of Geology, University of Warsaw, Żwirki i Wigury 93, 02-089, Warsaw, Poland; e-mails: r.mieszkowski@uw.edu.pl, se.mieszkowski@student.uw.edu.pl*
[2] *Polish Geological Institute – National Research Institute, Rakowiecka 4, 00-975 Warszawa, Poland; e-mail: kamwasilewski0@gmail.com*
[3] *Building Research Institute, 21 Ksawerów St., 02-656 Warsaw, Poland; e-mail: t.godlewski@itb.pl*

ABSTRACT:

Wasilewski, K., Mieszkowski, R,. Mieszkowski, S., and Godlewski, T. 2026. Integrating initial shear modulus (G_0) derived from seismic data with long-term deep-seated inclinometer displacements at selected Polish Outer Carpathian flysch landslides *Acta Geologica Polonica*, **76** (2), e85.

Landslide investigations have increasingly focused on integrating geotechnical monitoring with geophysical methods to improve the characterisation of internal slope processes and deformation mechanisms. This study presents a combined analysis of long-term deep-seated inclinometer displacements and seismic measurements conducted at selected landslides located in the Polish Outer Carpathian flysch. Two instrumented landslides were investigated using multi-year inclinometer monitoring covering periods of approximately 4–9 years, together with seismic refraction surveys. The initial shear modulus at very small strains (G_0) was derived from shear-wave velocity (V_s) and bulk density values calibrated using laboratory measurements, providing a quantitative indicator of subsurface stiffness variability. Vertical distributions of G_0 were compared with cumulative deep-seated displacements recorded by inclinometers, which allowed the identification of kinematic-mechanical deformation zones within the landslide bodies and their relationship to lithological and structural conditions. The results indicate that the integration of geophysical stiffness parameters with long-term inclinometer monitoring enables a more detailed delineation of zones characterised by different deformation behaviour. This approach supports the interpretation of deep-seated landslide structure in flysch terrains and provides a basis for further development of site-specific slope stability assessment and monitoring strategies.

Key words: Carpathian flysch; Landslide monitoring; Inclinometer measurements; Initial shear modulus; Shear wave velocity; Seismic refraction.

INTRODUCTION

Over the last two decades, landslide research has increasingly adopted integrated approaches that combine engineering geophysics, geotechnics, and remote sensing monitoring (e.g., satellite-based techniques) (Whiteley *et al.* 2019; Pazzi *et al.* 2019; Jongmans *et al.* 2021). Such integration enables the analysis of slope processes over a wide range of temporal and spatial scales. In their review, Whiteley *et al.* (2019) highlighted the need to integrate inclinometer data with geophysical measurements, including seismic

© 2026 Kamil Wasilewski, Radosław Mieszkowski, Stanisław Mieszkowski, Tomasz Godlewski. This is an open access article under the CC BY license (http://creativecommons.org/licenses/by/4.0/), which permits use, distribution, and reproduction in any medium, provided that the article is properly cited.

methods, stating that: "A key area for future development is the implementation of multiparametric monitoring with geotechnically coupled approaches. This can be achieved through better calibration of geophysical measurements with geotechnical data, and the establishment of threshold values for failure based on these outputs" The authors also emphasised that: „The establishment of site-specific geotechnical-geophysical relationships to obtain the subsurface spatial distribution of geotechnical properties, and the ability to monitor changes in these properties over time, is valuable to a wide range of end-users and stakeholders (Crawford and Bryson 2018**;** Merritt *et al*. 2016).

Jongmans *et al.* (2021) further stressed that geophysical investigations should be integrated with observations of ground movement, noting that: "They must be complemented by conventional (piezometric level, soil moisture and soil movement) and meteorological data for a complete understanding of the processes" and that: "These data are essential to improve our understanding of the geophysical response of landslides during their activation and the coupling between geophysical parameters and geotechnical properties"

The literature review presented by these authors includes several case studies that integrate electrical resistivity tomography (ERT) results with shallow displacement measurements (typically down to depths of 2.0–3.0 m below ground level), combined with GPS and stereophotogrammetric observations that record changes in ground surface morphology and electrode positions (Uhlemann *et al*. 2016). For the Monte Vecchio landslide, Mainsant *et al*. (2012) documented a decrease in apparent Rayleigh-wave velocity derived from ambient seismic noise correlations, which is interpreted as reflecting changes in shear-wave velocity (V_s), correlated with rainfall and landslide acceleration, followed by an increase in velocity during subsequent deceleration of movement.

Examples of multi-parameter investigations include so-called "landslide laboratories", where geophysical and geotechnical measurements are conducted simultaneously. Permanent landslide observatories operating in the United Kingdom and Austria provide long-term, multi-parameter datasets documenting landslide behaviour (Uhlemann *et al*. 2017; Whiteley *et al*. 2020; Stark *et al*. 2020; Luhn *et al*. 2023). More recently, distributed acoustic sensing (DAS) systems based on fibre-optic cables have gained attention, as they provide continuous profiles of ground strain along the cable length. However, this technique is characterised by limited depth resolution and interpretation challenges under complex geological conditions (Ouellet *et al*. 2024). Watlet *et al*. (2024) presented an innovative approach integrating ERT and DAS methods on a representative slope, confirming a relationship between soil moisture conditions and the initiation of deformation. An example of an integrated approach accounting for both temporal and spatial variability at a landslide located on a ski slope was presented by Marciniak *et al*. (2024).

Numerous studies have documented the integration of various parameters with shallow surface deformations recorded using GPS position changes (Calcaterra *et al*. 2011; Šegina *et al*. 2020), LiDAR surveys (Jaboyedoff *et al*. 2012; Perski *et al*. 2014; Peduto *et al*. 2021), unmanned aerial system (UAS) photogrammetry (Mugnai *et al*. 2023), low-cost MEMS-based shallow inclinometers (Fiolleau *et al*. 2023) and, more recently, InSAR techniques (Intrieri *et al*. 2020**,** Di Matteo *et al*. 2023**,** Peduto *et al*. 2021). In addition, individual case studies have employed multichannel analysis of surface waves (MASW) and microtremor measurements (HVSR) to develop integrated geological-seismic models (Seitone *et al.* 2025).

Although the international literature includes studies that partially combine geophysical data with inclinometer measurements, these investigations typically focus on short-term monitoring or shallow landslides and do not address deep inclinometer boreholes monitored over many years. No studies have yet been identified which comprehensively integrate long-term (approximately 4–9 years) deep-seated displacements measured using conventional inclinometers installed to depths of 20.0–30.0 m below ground level with profile-based distributions of elastic parameters (G_0, V_s) derived from seismic tomography. For the Polish Outer Carpathian flysch in particular, attempts to combine multi-year inclinometer records with elastic stiffness parameters of the ground are lacking. The present study addresses this gap by linking measured deep-seated, cumulative displacements with initial shear moduli (G_0), determined from seismic surveys for very small strain levels (10^{-6}-10^{-5}) together with shear-wave velocities V_s.

The need for such integration has been emphasised in the literature, where it has been suggested that combining geophysical and geotechnical data (e.g., inclinometer measurements) can significantly improve the understanding of landslide mechanisms (Pazzi *et al.* 2019). A quantitative approach is increasingly advocated, in which geophysical parameters are translated into geotechnical properties of landslide materials.

Several studies have used inclinometer measurements (deep-seated displacements) in combination with the initial shear modulus G_0 or shear-wave velocity V_s. For example, (Salciarini *et al.* 2022) employed inclinometer data to identify the slip surface and downhole (DH) seismic measurements to determine V_s and, indirectly, G_0 for numerical modelling purposes in a case study. In another example, a single inclinometer borehole monitored for only 1.5 years was used to calibrate geophysical survey results on an earthflow-type landslide, with the short monitoring period resulting from damage to the measurement installation (Bounab *et al.* 2025). In the case study by Huntley *et al.* (2019) inclinometers equipped with synchronous serial interface (SSI) and ShapeAccelArray (SAA) sensors were installed in boreholes and combined with MASW surveys to develop a comprehensive landslide model. However, a direct correlation between parameters was not described in detail. In a study conducted in the United States, Rahimi (2021) reported correlations between changes in V_s at the soil-bedrock contact and increases in cumulative displacements.

To date, no studies have been reported in Poland — particularly within the Carpathian flysch — that integrate, and correlate recorded deep-seated displacements with the small-strain shear modulus (G_0) and/or shear-wave velocities V_s. The only contributions addressing related issues are studies (Harba and Pilecki 2017) and (Harba *et al.* 2019), which attempted to integrate MASW and passive seismic interferometry results at the Just-Tęgoborze landslide with slip surface interpretations derived from geological engineering investigations. These studies also documented changes in V_s under varying moisture conditions. The study indicated the clear potential of seismic methods for landslide investigations in the Polish Carpathian flysch, but it did not include deep-seated inclinometer displacement data. The importance of seismic refraction profiling and electrical resistivity tomography for analysing the internal structure of landslides in the Carpathian flysch has also been highlighted by Ostrowski *et al.* (2013) and (Ostrowski *et al.* 2023). Although producing a landslide stability coefficient for the Carpathian flysch (Bestyński *et al.* 2017; Bestyński and Pacanowski 2025), it does not incorporate shear-wave velocity (V_s) or the shear modulus at very small strains (G_0).

The limited number of publications addressing these issues may be due to several factors. A common problem on active landslides is damage of monitoring installations, caused by jamming, blocking or bending of inclinometer casings within deformation zones and bedding-parallel faults, as well as angular offsets developing along slip surfaces during progressive movement, which can interrupt continuous observations. Uhlemann *et al.* (2016), Whiteley *et al.* (2020) and Jongmans *et al.* (2021) emphasised that projects integrating geophysical and geotechnical monitoring are relatively rare, mainly due to high costs, logistical challenges, and the limited availability of long-term inclinometer datasets. Such projects also require substantial instrumentation and the involvement of specialised teams from different disciplines, which can represent an organisational barrier.

In response to the limited number of studies combining elastic stiffness parameters of the ground medium, with deep-seated displacements in flysch landslides, this paper attempts to integrate geophysical and inclinometer data, enabling local calibration of the initial shear modulus (G_0) and the definition of shear-wave velocity (V_s) ranges associated with slope activity.

According to the relationship:

$$G_0 = \rho \cdot V_s^2,$$

where: G_0 = initial shear modulus in the very small-strain range (10^{-6}–10^{-5}); ρ = bulk density [kg/m^3]; V_s = shear-wave velocity [m/s]

The initial shear modulus at very small strains (G_0) incorporates information not only on the shear-wave velocity V_s (squared), but also on the bulk density of the ground medium ρ. In this way, (G_0) accounts for the mass per unit volume of the soil or rock, and thus reflects the inertial properties of the medium. Parameters obtained from seismic investigations (G_0, V_s) and laboratory tests (ρ) characterise the stiffness of the ground under elastic conditions and provide a basis for correlation with static geotechnical para- meters.

In engineering geotechnical practice, increasing emphasis is placed on ground characterisation using dynamic parameters. The most recent European Commission guidelines (Garin et al. 2024) for ground model development explicitly recommend the inclusion of the shear modulus at very small strains (10^{-6}–10^{-3}) and in situ shear-wave velocity (V_s) measurements when constructing ground models (Garin et al. 2024). Similarly, the second generation of Eurocode 7 (EN-1997) introduces the requirement that ground models documented at the investigation stage should include seismic parameters of the ground, such as G_0 and field-derived V_s values. This demonstrates that the application of engineering seismic methods, together with established correlations between dynamic and static soil moduli (Hardin and Drnevich 1972, Atkinson 2000) constitutes a fundamental basis for calibrating numerical models used in the design of landslide stabilisation and mitigation measures.

STUDY AREA

The Mała landslide is located in the village of Mała (Ropczyce municipality, Ropczyce-Sędziszów County) in the Podkarpackie Voivodeship. The Słotowa landslide is situated in the village of Słotowa (Pilzno municipality, Dębica County) in south-eastern Poland (Podkarpackie Voivodeship). The most important characteristics of both study areas are summarised below (Tab. 1).

Both landslides are considered representative for the investigated problem because they are characterised by long-term inclinometer monitoring records, continuous or recurrent displacement activity over extended periods, and well-documented subsurface conditions. The sites include borehole data with known lithological profiles, as well as laboratory-derived physical parameters (e.g., bulk density), enabling reliable calibration of geophysical results. The selected landslides are characterised by sustained or recurrent kinematic activity, which is relatively uncommon among monitored sites. Although several dozen landslides are monitored within the SOPO programme in Poland, many of them remain inactive or exhibit only episodic displacement in long-term records. Therefore, the selection was based on the availability of consistent, long-term datasets and clearly expressed displacement activity, which are essential for the integration of stiffness parameters with deep-seated deformation. The analysis of cumulative deep-seated displacements, based on four inclinometer columns (two at each landslide) and referenced to the results of geophysical investigations covers approximately 4–9 years of observations. Previous observations, literature data, and archived monitoring records indicate that landslides developed within the Polish Carpathian flysch are characterised by long-term, very slow movements (up to several tens of millimetres per year) and are closely linked to changes in pore pressure conditions, including groundwater level fluctuations and atmospheric precipitation (Warmuz and Nescieruk 2019).

Parameter	**Mała landslide**	**Słotowa landslide**
SOPO ID	18-15-033-78473	18-03-065-071897
Geographic region	Western Outer Carpathians	Western Outer Carpathians
Tectonostratigraphic unit (nappe)	Skole	Silesian
Landslide type	translational–rotational	translational–rotational
Activity status	active	active
Length [m]	400	625
Width [m]	455	390
Area [ha]	8.44	24.07
Elevation range (Hmin–Hmax) [m a.s.l.]	250–300	280–370
Relative height difference (ΔH) [m]	50	90
Slope aspect	N	SE-SSE
Dominant lithology	silty clays and clays (weathered flysch)	clayey shales (flysch), locally with sandstone interbeds.
Lithological composition [%]	silty clays and clays: 90–95%, weathered flysch (claystone): 5–10%, sandstones (fragments) <5%	shales: 80-85%, sandstones: 0–20%, soils: 5–15%.
Bedding dip (SMGP/surface data) [°]	No reliable information	No reliable information
Structural setting	strongly tectonized flysch with thrust and fault zones	strongly tectonized flysch with thrust and delamination (shear) zones.
Hydrogeological conditions	shallow groundwater, seasonal fluctuations	shallow groundwater, seasonal fluctuations
Main triggering factors	rainfall, snowmelt	rainfall, snowmelt
Number of inclinometer boreholes	2	2
Inclinometer depth [m]	21.0–27.0	18.5–28.0
Analysis period (inclinometric data)	2011–2015 (Mała 1) 2015–2024 (Mała 2)	2016–2024 (Słotowa 1) 2017–2024 (Słotowa 2)
Measurement frequency	typically, twice per year (spring–autumn)	
Groundwater table depth [m b.g.l.]:	2.0–3.0 ($\Delta h \leq 1.8$ m)	0–0.5; 4.0–6.0 ($\Delta h \leq 2.0$ m)

Tab. 1. Main characteristics of the investigated landslides.

METHODOLOGY

Field investigations included seismic measurements carried out by the authors of this study, as well as the use of monitoring data obtained within the framework of the national Landslide Counteracting System (SOPO).

Seismic refraction and seismic tomography surveys were conducted along seven profiles, four of which were located at the Słotowa landslide and three at the Mała landslide. The orientation of the profiles with respect to the landslide morphology is shown in Text-fig. 1. The seismic profiles were designed to provide coverage across the main landslide body and to pass as close as possible to the inclinometer boreholes. Their layout was constrained by landslide morphology, accessibility, vegetation cover, and acquisition conditions. Where possible, the profiles were oriented consistently with the dominant displacement direction and the inclinometer layout. Data acquisition was performed using a 24-channel seismograph connected to horizontal geophones with a natural frequency of 4.5 Hz, spaced at 5 m intervals, resulting in a total profile length of approximately 115 m. Compressional waves (V_p) were generated by impacts of a 9 kg hammer striking a steel plate placed on the ground surface. Shear waves (V_s) were generated by hammer impacts on a steel anvil rigidly coupled to the ground, with signal recording performed using horizontal geophones (4.5 Hz) oriented according to the polarisation direction of the S-wave (Text-fig. 2). Five shot points were deployed along each profile, and the recorded signals were stacked eight times to improve the signal-to-noise ratio. A multi-shot acquisition scheme was applied, in which the source position was shifted every four geophones, combining the advantages of end-on and split-spread configurations and ensuring relatively uniform coverage of first arrivals.

The processing workflow included signal filtering, picking of first-arrival travel times, and tomographic inversion performed using the Geogiga Seismic Pro software (DW Tomo module), which implements a two-dimensional first-arrival traveltime tomography algorithm. The average root mean square (RMS) error of the inversion was below 1.5 ms. The resulting P-wave and S-wave velocity fields (V_p, V_s) were used to calculate dynamic (initial) parameters of the soil-rock medium, including the initial shear modulus defined as $G_0 = \rho \cdot V_s^2$. The values of the initial shear modulus G_0 derived from seismic refraction surveys correspond to the very small strain range (10^{-6}–10^{-5}) and may be considered comparable to the maximum shear modulus Gmax defined for very small strains in laboratory BET/RCT tests. This interpretation is consistent with the G_{max}–G_0 relationship discussed in Section 4.4.2 by (Godlewski and Szczepański, 2015).

In addition, the dynamic Young's modulus (E_d), the initial constrained (oedometric) modulus (M_0), and the dynamic Poisson's ratio (ν_d) were calculated from V_p i V_s. In this study, however, these parameters were used only for auxiliary purposes, including quality control and lithological interpretation. The primary analysis focused on the coupling between cumulative displacements and the initial shear modulus G_0 (derived from V_s). The notation adopted follows common practice in geotechnics and geophysics, where G_0 and M_0 denote initial (very small strain) shear and constrained moduli, respectively, while Ed and νd represent the dynamic equivalents of Young's modulus and Poisson's ratio.

For the seismic cross-sections S1–S2 and S4–S5 the presence of so-called near-surface "dead zones" should be taken into account. These zones, extending to depths of approximately 2.0–3.0 m, are characterised by reduced resolution and increased uncertainty, resulting from limited ray coverage and the geometry of the acquisition layout. Profiles S3, S6 i S7 which were not associated with inclinometer measurements, served a supplementary role. They were used comparatively to identify variations in the internal structure of the landslides and to support the interpretation of the remaining profiles. Bulk density (ρ) was determined in the laboratory for 38 samples (19 from each landslide; Institute of Geotechnics 2010a, 2010b) using the cutting-ring method and triaxial sample measurements, yielding values in the range of 1820–2350 kg/m³. The observed variability of bulk density values reflects the heterogeneous lithology of the flysch sequence, including interbedded sandstones and shales. The results for each sample are presented in the column titled "average bulk density [kg/m³]" (example: Text-fig. 3). The bulk density values obtained from laboratory samples were averaged and used to define local empirical ranges of correlation with shear-wave velocities (V_s) derived from seismic inversion. This local calibration enabled refinement of the elastic parameters and provided a more realistic representation of subsurface stiffness. The calibrated density values, assigned to corresponding depths and V_s values, were subsequently used in the calculation of G_0.

Data on deep-seated displacements were obtained from inclinometer monitoring conducted

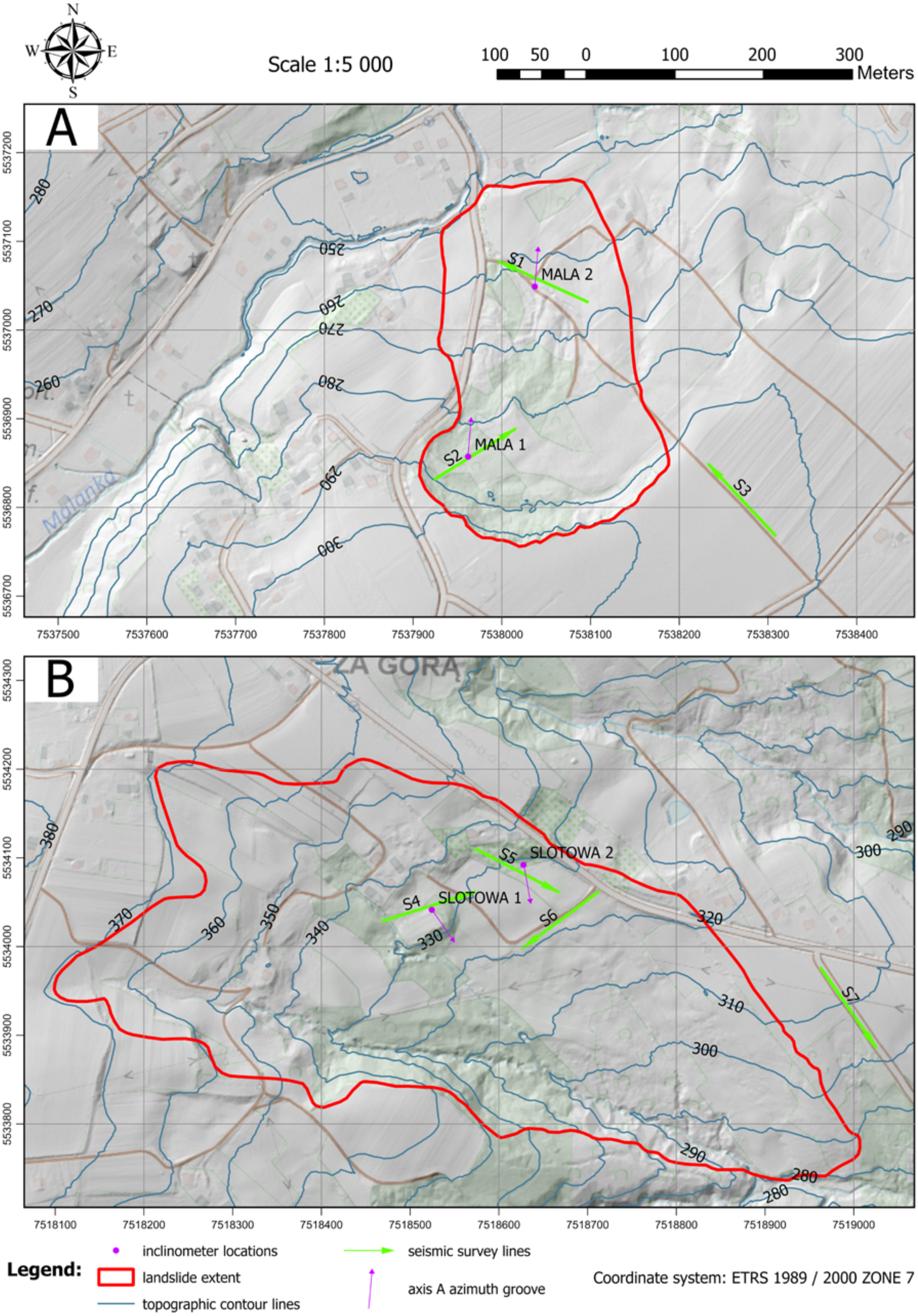

Text-fig. 1. Landslide extent and distribution of seismic survey lines and inclinometer boreholes locations in the Mała (A)-Słotowa (B) areas.

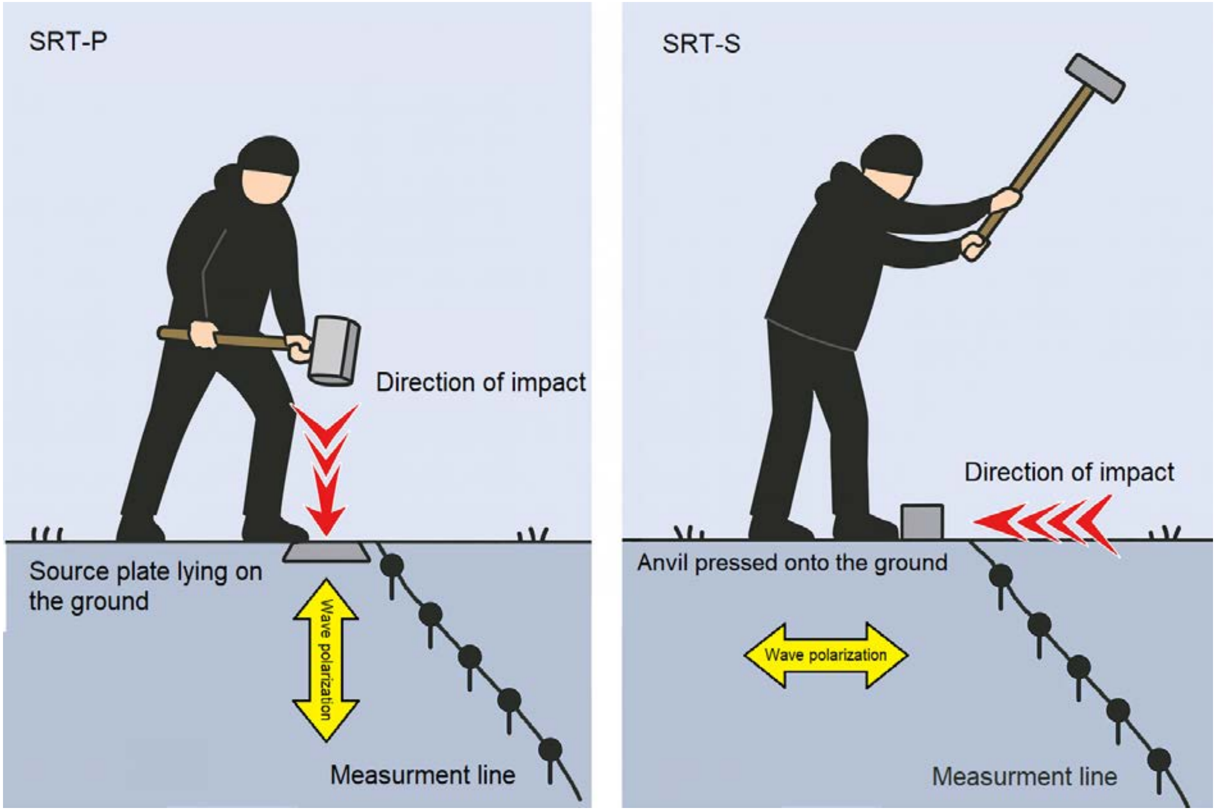

Text-fig. 2. Data acquisition methodology for seismic refraction tests (SRT-P and SRT-S). In this study, SRT-S measurements constitute the primary dataset used for stiffness (G0) interpretation, whereas SRT-P data were acquired for supplementary characterization of subsurface conditions.

within the SOPO programme at the Mała and Słotowa landslides (PGI-NRI 2016, Nescieruk *et al*. 2024a, 2024b). At both sites, inclinometer columns were installed in two perpendicular measurement directions (A-A' and B–B'), with the A–A' axis aligned with the dominant direction of landslide movement. Measurements were carried out using a digital RST inclinometer probe, lowered at 0.5 m intervals along the entire borehole depth. Results are presented as displacement profiles as a function of depth below ground level (m b.g.l.), expressed in millimetres. For the Mała 1 borehole, cumulative displacement analysis was restricted to the 2011–2015 monitoring period due to shearing of the inclinometer column after October 2015. Although measurements were performed along both axes, further quantitative analysis was restricted to the A–A' axis, representing the principal movement direction, as displacements recorded along the B–B' axis were minor and did not show consistent trends relevant for the interpretation. The declared accuracy of the inclinometer system is ±1–3 mm and was taken into account in the analyses. The complete original inclinometer displacement curves for both measurement axes (A–A' and B–B') are provided in the Supplementary Material (SUP3–SUP6).

Integrated depth profiles were developed by directly combining: (i) cumulative inclinometer displacements as a function of depth, (ii) the distribution of the initial shear modulus G_0 w derived from shear-wave velocity (V_s) and adopted bulk density values, and (iii) lithological information from borehole logs. Values of G_0 were assigned to inclinometer depths based on the spatial relationship between inclinometer locations and seismic profiles. Cumulative displacements were analysed both as final values and in terms of their temporal increments, which allowed the characterisation of displacement kinematics.

On this basis, three kinematic-mechanical deformation zones were distinguished:

(A) an active zone, characterised by high cumulative displacements and low G_0 values,

(T) a transitional zone, comprising intervals of intermediate stiffness and variable kinematic behaviour, which, depending on local conditions, may represent deformation transitional between localised

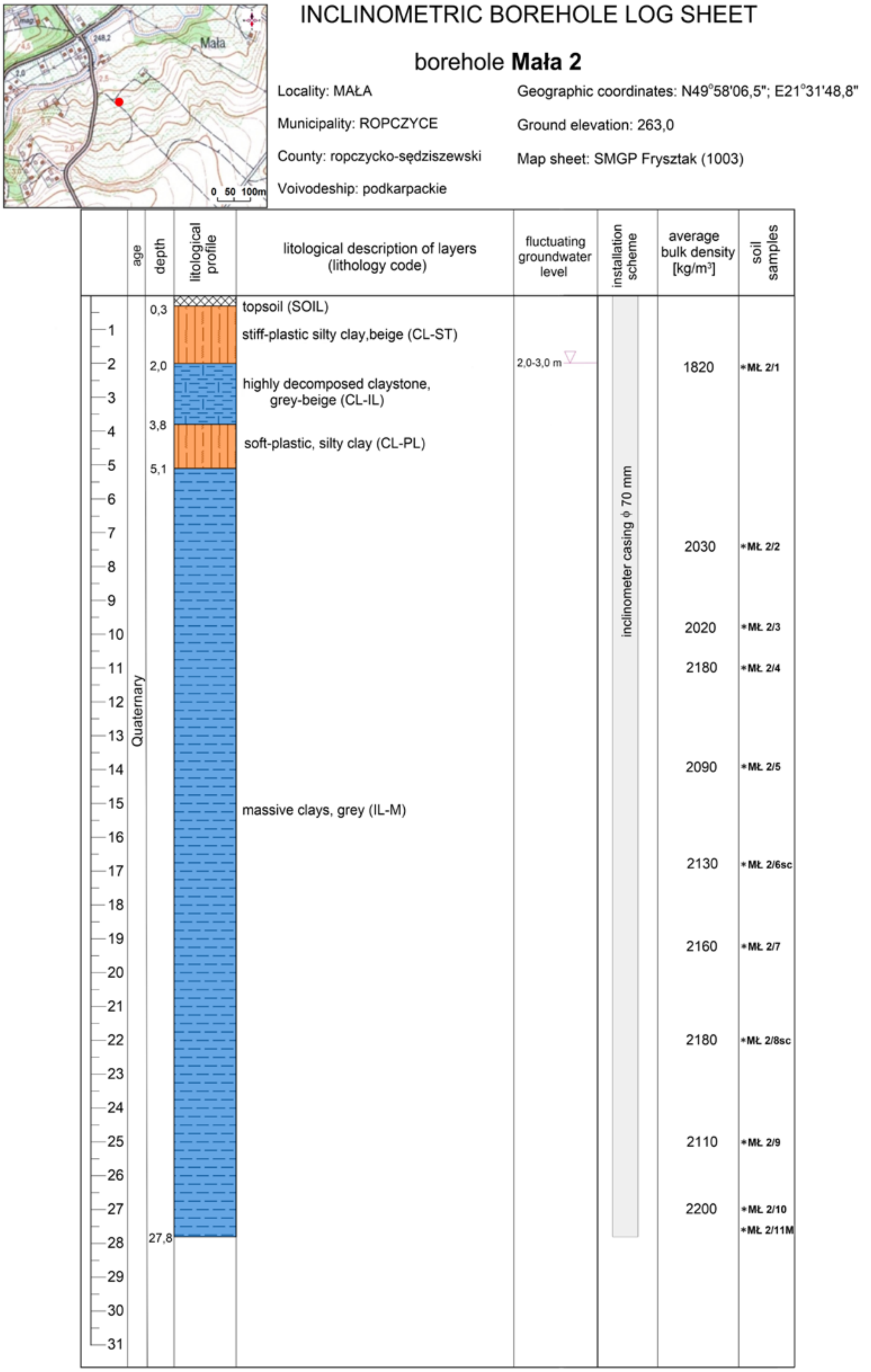

Text-fig. 3. Inclinometric borehole log Mała 2 with lithology, groundwater table fluctuation range, average bulk density, and sampling depths (own elaboration based on Nescieruk *et al.* 2010; Institute of Geotechnics 2010a).

shear and partially coherent movement within fractured flysch units (T-A), or a relictually deformed package (T-R)

(QS) a quasi-stable zone, in which cumulative displacements are negligible and G_0 values reach levels characteristic of mechanically stiff substrata.

RESULTS

Inclinometer borehole logs describing lithology, including standardised lithology codes assigned to individual layers (e.g., SOIL, CL-ST, IL-M), together with laboratory bulk density results for individual samples from the MAŁA landslide, are presented in Text-fig. 3 and Supplementary Figure SUP1. The corresponding distribution of initial (dynamic) shear modulus values (G_0) along seismic tomography profiles S1 and S2 is shown in Text-fig. 4.

Equivalent lithological logs and bulk density results for the SŁOTOWA landslide are presented in Text-fig. 5 and Supplementary Figure SUP2, while the distribution of G_0 values along seismic tomography profiles S4 and S5 is shown in Text-fig. 6. At the locations of inclinometer installations (x = 60 m), lithological columns derived from inclinometer borehole logs are superimposed on the tomographic sections.

At both the Mała and Słotowa landslides, the distributions of G_0 along the analysed profiles (Mała: S1 and S2; Słotowa: S4 and S5) exhibit a similar, layered subsurface structure. Low G_0 values occur in the near-surface zone, corresponding to low-stiffness colluvial materials, followed by a marked increase in G_0 with depth towards mechanically stiffer units. The comparison of G_0 profiles with inclinometer data indicates that the highest deformations are generally concentrated in zones of reduced G_0 values, while deeper sections are characterised by higher stiffness. However, a deviation from this pattern is observed in the Słotowa 1 profile, where elevated G_0 values are accompanied by significant displacements. Moreover, the adjacent Słotowa 1 and Słotowa 2 profiles, despite their close spatial proximity, show different depths of deformation concentration, indicating a spatial variability of deformation within the analysed landslide. These observations form the basis for further integration of geophysical and inclinometer data, enabling a quantitative assessment of the relationship between low-stiffness zones and the concentration of deformation, as presented in subsequent analyses.

The main synthesis of results is provided by the integrated depth profiles entitled: Integrated depth profiles of cumulative inclinometer displacement and very small-strain shear modulus (G_0) with lithological units (multiplot) — Text-fig. 7. For both landslides, three principal kinematic-mechanical deformation zones were distinguished on the basis of the coupling between cumulative inclinometer displacements and stiffness parameters (G_0): an active zone (A), a transitional zone (T-A, T-R), and a quasi-stable zone (QS). These deformation zones were defined as depth intervals delineated based on: (i) the kinematic characteristics of displacements (magnitude, distribution, and temporal evolution) and (ii) the mechanical state of the medium described by G_0 (very small-strain stiffness) and lithology. The transitional zone may occur in two variants: as an active transitional zone (T-A), characterised by ongoing kinematic activity, or as a relict transitional zone (T-R), exhibiting intermediate stiffness but no significant displacement increases during the analysed monitoring period. It should be emphasised that the kinematic-mechanical zones defined in this study are broader interpretative domains and should not be equated directly with narrow shear zones identified from inclinometer curves. The latter may have thicknesses of only 1–2 m and mark the main displacement concentration, whereas the transitional zones reflect wider intervals of changing stiffness, lithology and residual or ongoing deformation.

The Mała 1 profile shows an active zone extending from the ground surface to a depth of approximately 7.5 m (depending on the inclinometric profile). This zone is characterised by the highest cumulative displacements, reaching approximately 70–80 mm. It corresponds to a package of cohesive soils and weathered materials (SOIL, CL-ST, IL-M), characterised by low G_0 values (40–60 MPa). Displacements are clearly concentrated within this part of the profile, indicating dominant deformation activity in the near-surface zone. Below this interval, a transitional zone (T-R) occurs between approximately 7.5 and 17 m depth, where cumulative displacements systematically decrease from values of about 9 mm to approximately 2–3 mm with increasing depth. At the same time, a marked increase in G_0 is observed, from approximately 60 MPa to values exceeding 200 MPa. This T-R zone is composed mainly of massive clays (IL-M). In the lower part of the profile, cumulative displacements approach negligible values (<2 mm), while G_0 reaches high values (approximately 250–350 MPa), typical of stiff, less-deformed packages of massive clays (IL-M).

The Mała 2 profile exhibits a similar pattern. high cumulative displacements of approximately 50–60 mm are observed, concentrated within plastic soils (CL-ST, CL-IL, CL-PL). G_0 values within this interval are very

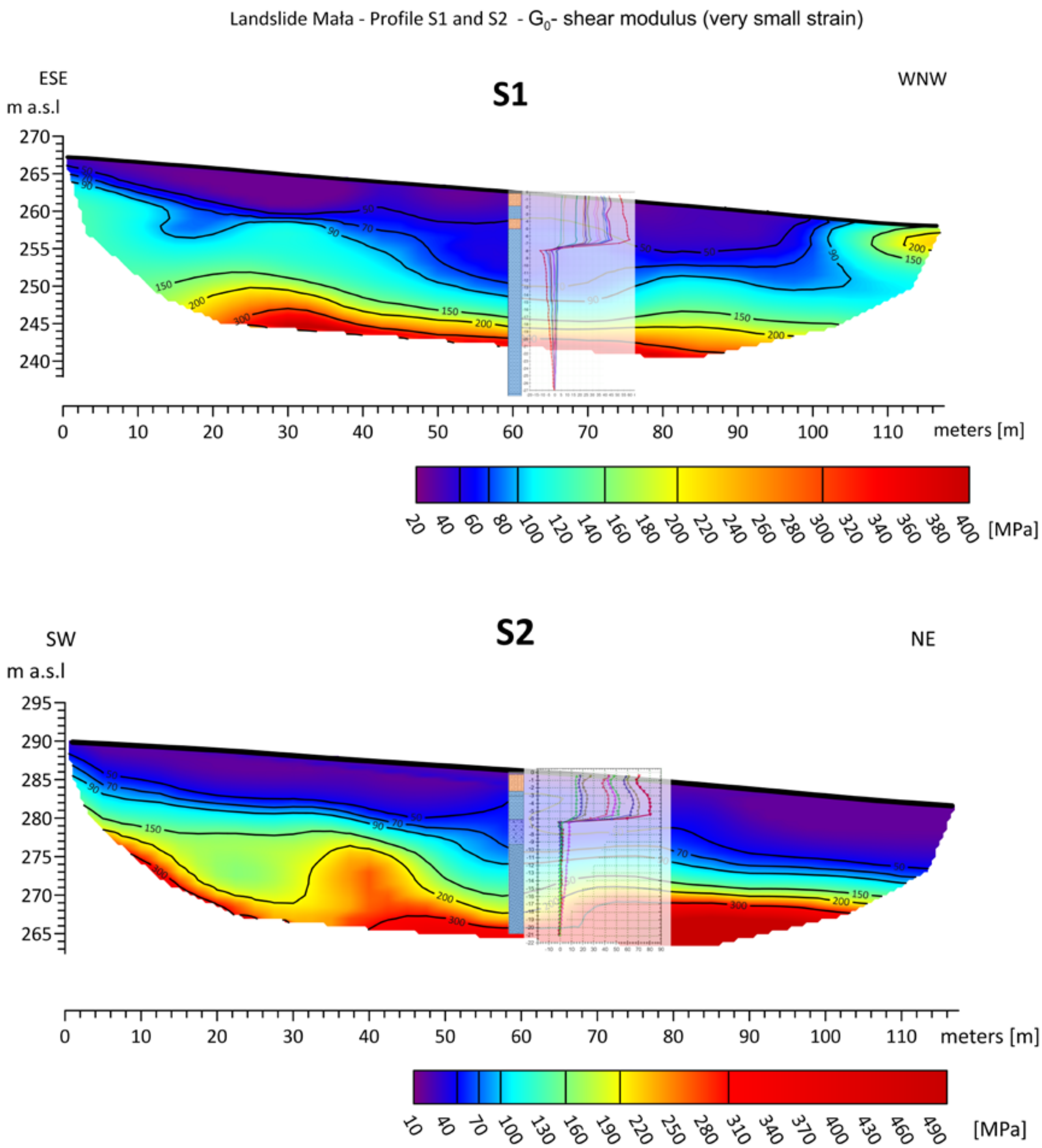

Text-fig. 4. Distribution of the very small-strain shear modulus (G_0) along seismic profiles S1 and S2 at the Mała landslide, combined with the inclinometer location, lithological column, and cumulative displacement profiles.

low (approximately 40–55 MPa), indicating a significantly weakened and deformation-prone medium. The active zone terminates at a depth of approximately 8.0–8.5 m. Below this depth, a transitional zone (T-R) extends down to approximately 18 m, where displacements-analogous to those observed in the previous inclinometer-rapidly decrease from values of about 10 mm to only a few millimetres with depth. Concurrently, a pronounced increase in the initial shear modulus G_0 is observed within massive clays (IL-M) from approximately 60 MPa to 220–230 MPa, indicating a progressive increase in stiffness. Below approximately 18 m depth, cumulative displacements are negligible, while G_0 reaches high values (approximately 240–350 MPa). This part of the profile represents mechanically stiff, quasi-stable landslide substratum.

The Słotowa 1 profile is characterised by an active zone developed within weathered materials (SOIL,

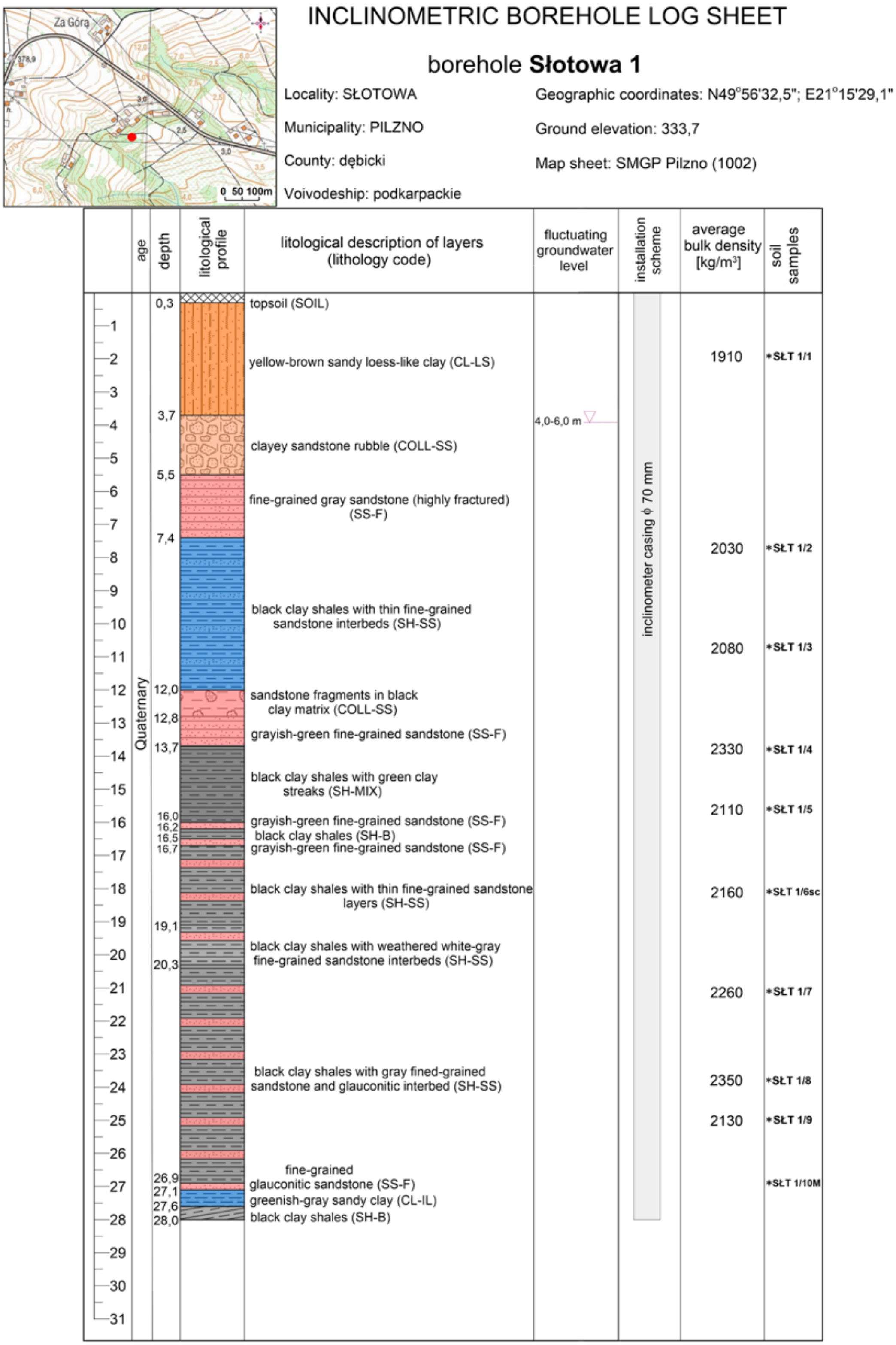

Text-fig. 5. Inclinometric borehole log Słotowa 1 with lithology, groundwater table fluctuation range, average bulk density, and sampling depths (own elaboration based on Nescieruk *et al.* 2014; Institute of Geotechnics 2010b).

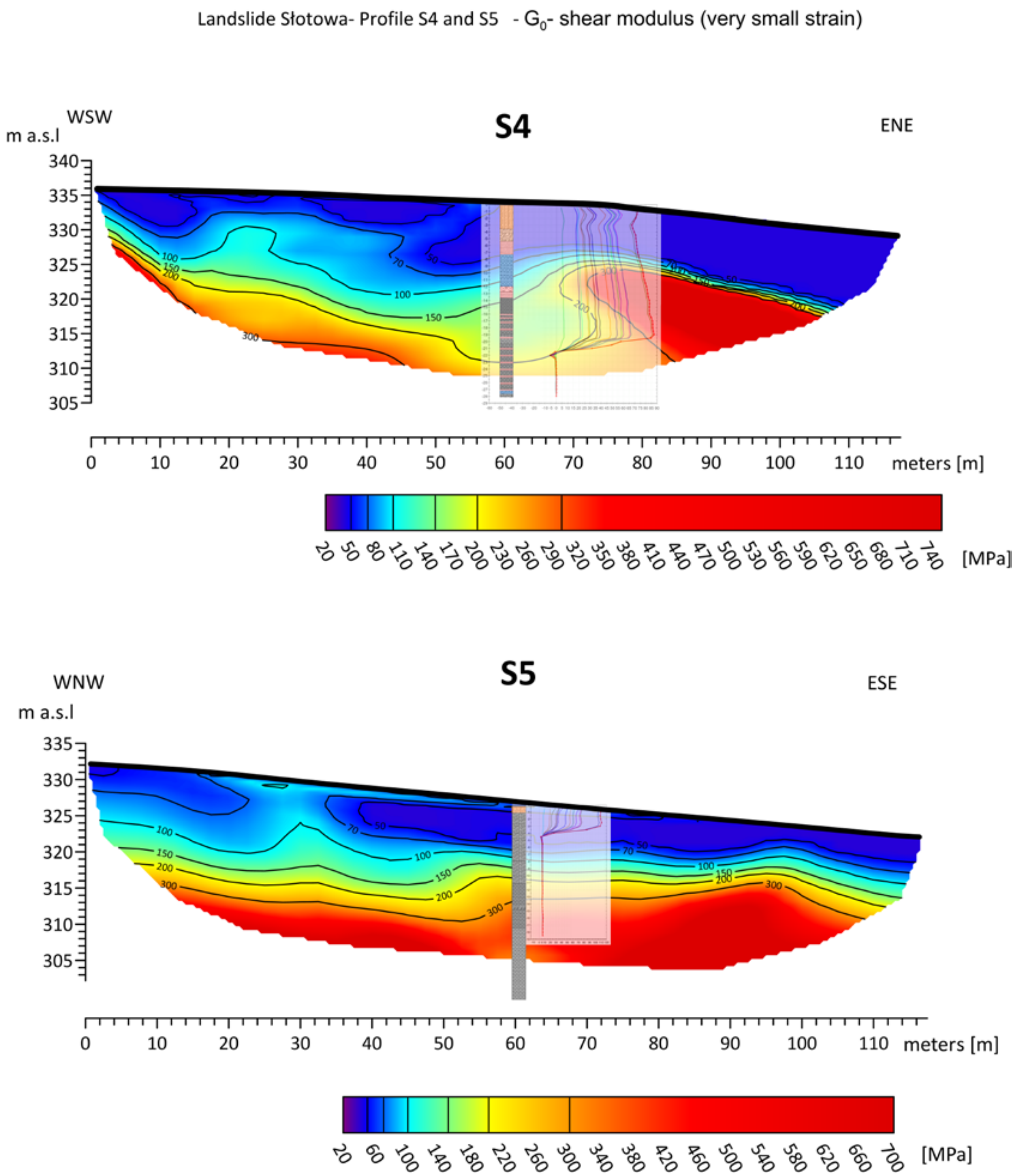

Text-fig. 6. Distribution of the very small-strain shear modulus (G_0) along seismic profiles S4 and S5 at the Słotowa landslide, combined with the inclinometer location, lithological column, and cumulative displacement profiles.

CL-LS, COLL-SS) down to a depth of approximately 7.5 m. Within this zone, large cumulative displacements of approximately 70–80 mm are recorded. The medium is characterised by low initial shear modulus values, on the order of 50–60 MPa, indicating high susceptibility to deformation. Between approximately 7.5 and 23 m depth, an active transitional zone (T-A) is identified, exhibiting a kinematic behaviour distinct from that of the active zone. Cumulative displacements remain significant and continue to increase over time, while the medium displays noticeably higher mechanical stiffness. This zone is primarily composed of flysch units with sandstone interbeds (SS-F, SH-SS, SH-MIX). G_0 values increase from approximately 70–80 MPa to 180–190 MPa. The increase in stiffness does not result in a cessation of kinematic activity, suggesting that deformation within this interval is complex and involves both localised

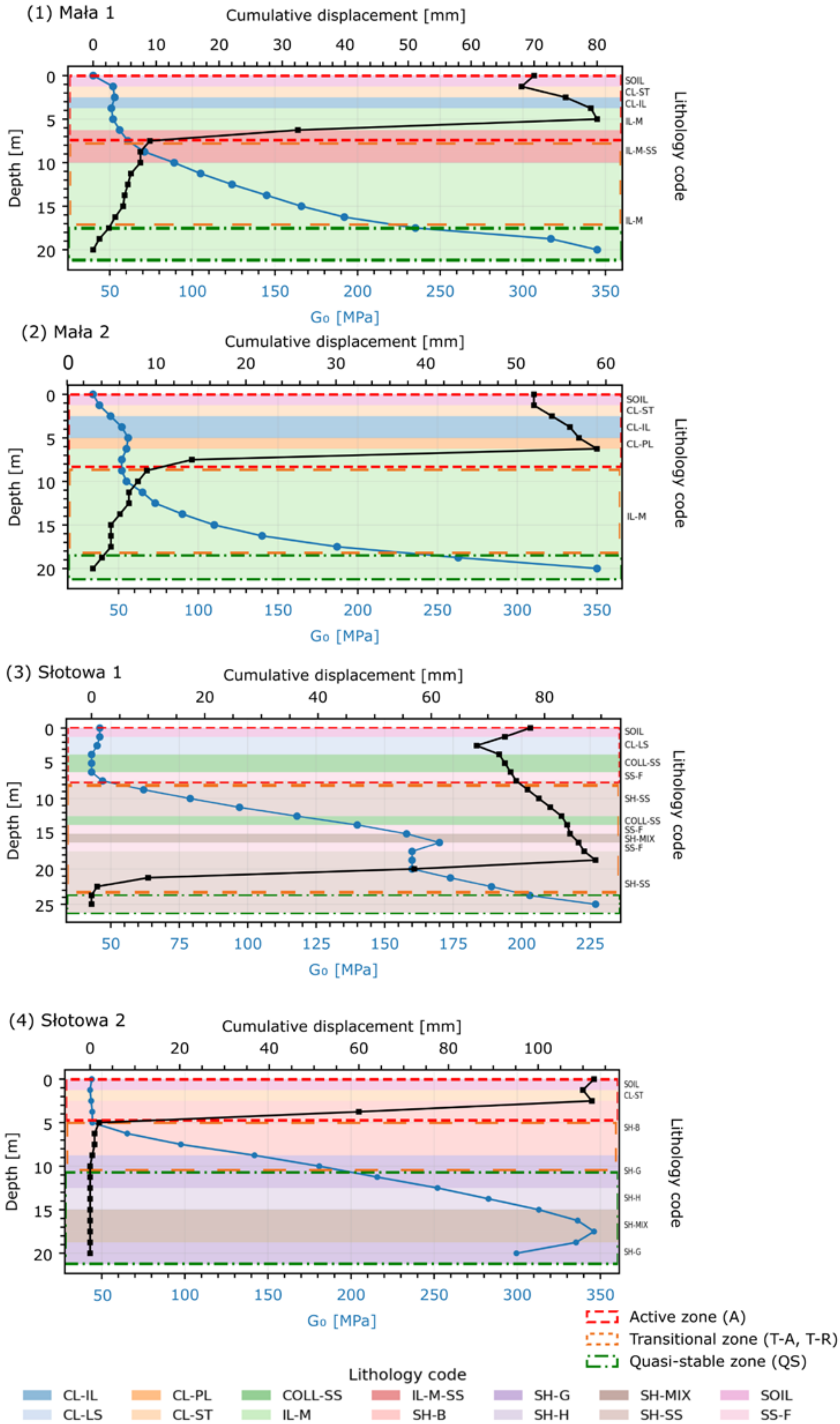

Text-fig. 7. Integrated depth profiles of cumulative inclinometer displacement and very small-strain shear modulus (G_0) with lithological units – multiplot.

shear and partially coherent movement within a mechanically stiffer, strongly fractured flysch medium. For this reason, this interval is classified as an active transitional zone (T-A), understood as mechanically transitional but kinematically active. Below approximately 23–23.5 m depth, cumulative displacements decrease to values close to 0 mm, while G_0 values increase to approximately 200–220 MPa, typical of a stiff and less-deformed substratum. This zone is classified as quasi-stable.

The Słotowa 2 profile differs slightly, with the active zone extending from the ground surface to a depth of approximately 5 m. Within this zone, very high cumulative displacements of up to approximately 110 mm are recorded, concentrated in cohesive soils and weathered shales (SOIL, CL-ST, SH-B). G_0 values are very low (approximately 45–55 MPa), indicating a strongly weakened, deformation-prone medium. Below this interval, a transitional zone (T-R) occurs in which cumulative displacements over the analysed nine-year monitoring period are negligible or close to zero. At the same time, a gradual increase in G_0 is observed, from approximately 60 MPa to values of about 180-200 MPa, associated with a transition into weathered, plastic clay shales (SH-G, SH-H). At a depth of approximately 11 m, a quasi-stable zone is identified. Cumulative displacements remain negligible, while G_0 increases sharply to values of approximately 300–340 MPa. This part of the profile corresponds to a stiff, quasi-stable landslide substratum.

DISCUSSION

Based on the comparative analysis of seismic and inclinometer data, the following discussion focuses on the relationships between elastic stiffness parameters and landslide kinematics. In Poland, and particularly within the Carpathian flysch, there is currently no commonly adopted subsurface classification of kinematic-mechanical deformation intensity that explicitly relates long-term cumulative inclinometer displacements to ground stiffness expressed by the initial shear modulus G_0. In some engineering-geological studies (e.g., Kos 2021) active slip surfaces and relatively rigid "block-like" zones are identified; however, no attempt has been made to standardise terminology or to define quantitative stiffness-based criteria for such divisions.

At the Mała landslide, where two inclinometer boreholes were analysed, G_0 values show a very good mutual correspondence both between the seismic profiles and in relation to the recorded displacement. Active and transitional zones occur at similar depths, and the threshold values of G_0 characterising these zones are highly consistent. This indicates that, in this case, elastic stiffness parameters adequately reflect the actual distribution of kinematic-mechanical deformation zones and support the internal consistency of the three-zone model under relatively homogeneous lithological conditions. A different situation is observed at the Słotowa landslide. Despite comparable values of the initial shear modulus G_0 along adjacent profiles (Słotowa 1 and Słotowa 2), distinctly different kinematic states were recorded within the transitional zone. In the Słotowa 1 profile, this zone is interpreted as reflecting complex deformation within fractured flysch layers, involving both localised shear and partially coherent movement, whereas in the Słotowa 2 profile it is interpreted as a mechanically transitional but relictually deformed (T-R) package of plastic materials, characterised by only negligible displacements during the analysed monitoring period.

The example of the T-A zone in the Słotowa 1 profile demonstrates that, under Carpathian flysch conditions, an increase in mechanical stiffness does not necessarily imply the cessation of kinematic activity, and that deformation may also persist within mechanically stiffer and strongly fractured flysch units. Despite the promising results obtained, this study is subject to several important limitations. First, due to the limited number of investigated sites (only two landslides with a total of four inclinometer columns), the potential for generalisation is restricted. The threshold values of the initial shear modulus G_0 and shear-wave velocity V_s (presented in the Conclusions and Future Research Perspectives section), should therefore be regarded as local and preliminary. Although literature data (Harba *et al.* 2019) suggest that a transition to less weathered substratum at V_s values of approximately 340 m/s is realistic, the results indicate that locally the velocities may be slightly lower, approximately 310-330 m/s. Further investigations at additional Carpathian landslides representing different lithological units are planned in order to examine threshold values under varying geological conditions.

In addition, uncertainties of both measurement and methodological origin must be considered. In particular, seismic profile S5 (Text-fig. 1) in the vicinity of the Słotowa 2 inclinometer (Text-fig. 6, Supplementary Material SUP 2) was offset by approximately 7.5 m relative to the measurement column, introducing uncertainty related to the spatial interpolation of G_0 values. Furthermore, the accuracy of inclinometer measurements (±1–3 mm) and the limited resolution of seismic methods — especially the presence of near-surface "dead zones" extending to depths of approximately 2.0–3.0 m with reduced reliability, as well as an average tomographic inversion misfit below 1.5 ms — affect the overall precision of the results. The G_0 values were also determined indirectly, based on tomographic inversion models and bulk density calibration, which involves additional assumptions and introduces further uncertainty. All these factors should be taken into account when interpreting the results and delineating deformation zones within the landslide bodies.

CONCLUSIONS AND FUTURE RESEARCH PERSPECTIVES

This paper constitutes the first part of a broader research programme covering different lithological and tectonic units of the Carpathian flysch nappes. The study is focused on a qualitative-quantitative analysis of the relationship between the initial shear modulus (G_0) and long-term inclinometer displacements, which enabled the integration of geophysical and geotechnical measurements and the preliminary delineation of kinematic-mechanical deformation zones (Text-fig. 7). The results indicate that the integration of geophysical data (G_0) with physically recorded cumulative displacements allows the definition of local ranges of elastic stiffness parameters corresponding to individual kinematic-mechanical deformation zones.

For the Mała landslide, the following threshold values were identified:

– active zone: G_0 < 50–60 MPa, V_s < 170–180 m/s,
– transitional zone: G_0 from 60 to 240–250 MPa, V_s = 180–330 m/s,
– quasi-stable zone: G_0 > 240–250 MPa, V_s = 330–350 m/s.

For the Słotowa landslide, differences between profiles Słotowa 1 and Słotowa 2 were observed, with the following range:

– active zone: G_0 < 55 MPa, V_s < 165–170 m/s,
– transitional zone: G_0 from 55 to 190–200 MPa, V_s = 170–310 m/s,
– quasi-stable zone: G_0 > 200 – 220 MPa, V_s > 310–320 m/s.

Comparison of the results indicates that G_0 values of the order of 50–60 MPa represent a characteristic range for shallow, active colluvial materials at the investigated landslides. In contrast, shear-wave velocitiesj V_s in the range of approximately 310–350 m/s (corresponding to G_0 values of about 200–250 MPa mark the transition to a mechanically stiff, quasi-stable substratum. The comparision of cumulative displacements with G_0 values enables comparison of the deformation potential between different lithological units within the very small-strain range. Accordingly, G_0 and V_s may be treated as indicators of the susceptibility of the ground medium to the initiation and concentration of deformation. The integration of geophysical data with long-term inclinometer monitoring provides a tool for the preliminary assessment of the mechanical equilibrium state of slopes and supports decisions related to monitoring design. In practice, zones characterised by low G_0 values may indicate areas requiring densification of inclinometer networks or the application of local stabilisation measures.

The presented parameter ranges should be regarded as local and preliminary, limited to the lithological and structural conditions of the analysed Carpathian flysch landslides. With the expansion of the measurement database to include additional lithological units, it will be possible to further evaluate threshold values under different geological conditions. The present study represents the first quantitative attempt to integrate multi-year inclinometer displacement data with very small-strain elastic stiff- ness parameters (G_0) in Carpathian flysch conditions, providing a reference framework for future investigations in other lithological units. The applied procedure for integrating geophysical and inclinometer data is repeatable and may be transferred to other flysch landslides and different geological environments, provided that local calibration is performed, and long-term deep-seated displacement data are available. While the methodology constitutes a general analytical framework, the resulting threshold values require site-specific verification in each case.

Supplementary Material

Supplementary Figures SUP1–SUP2 present detailed inclinometric borehole logs for Mała 1 and Słotowa 2, including lithology, groundwater conditions, and inclinometer installation geometry. Supplementary Figures SUP3–SUP6 provide the complete original inclinometer displacement records for both measurement axes. The supplementary materials will be available online after publication at DOI: 10.5281/zenodo.20820474.

Acknowledgments

This work received support from the Excellence Initiative – Research University (IDUB), project No. BOB-IDUB-622-492/2025. The authors acknowledge the availability of inclinometric and monitoring data collected within the national SOPO program of the Polish Geological Institute – National Research Institute (PGI–NRI).

REFERENCES

Atkinson, J.H. 2000. Non-linear soil stiffness in routine design. *Geotechnique*, **50** (5), 487–508.

Bestyński, Z., Pacanowski, G. and Sieiński E. 2017. Geophysical investigation and geotechnical classifications for stability assessment of Carpathian flysch slopes. *Przegląd Geologiczny*, **65** (10/2), 717–724. [in Polish].

Bestyński, Z. and Pacanowski, G. 2018. Ranking of geotechnical rock mass classifications and geophysical survey methodology for assessing tunneling conditions and slope stability in the Flysch Carpathians. In: Majer, E., Sokołowska, M., Frankowski, Z. (eds.), Principles of Geological and Engineering Documentation (in the Light of Eurocode 7 Requirements), PGI–NRI, Warsaw, pp. 99–109. [in Polish].

Bounab, A., El Kharim, Y., El Hamdouni, R., Sahrane, R. and Ourdaras, L. 2025. Multidisciplinary investigations of earthflow processes in the differential erosion furrows morphostructural unit, Northern Rif (Morocco): case study of the Seikha landslide. *Natural Hazards*, **121** (11): 12551–12574.

Calcaterra, S., Cesi, C., Di Maio, C., Gambino, P., Merli, K., Vallario, M. and Vassallo, R. 2011. Surface displacements of two landslides evaluated by GPS and inclinometer systems: a case study in Southern Apennines, Italy. *Natural Hazards*, **61** (1): 257–266.

Crawford, M.M. and Bryson, L.S. 2018. Assessment of active landslides using field electrical measurements. *Engineering Geology*, **233**, 146–159.

Di Matteo, L., Cardinali, R., Cerboni, V., Guadagnano, F., Piagnani, G., Ribaldi, C., Sotera, B.M. and Cencetti C. 2023. Integrated approaches for field mapping by traditional investigation and satellite PSInSAR data: Results from the Montemartano landslide (Central Italy). *Remote Sensing*, **15** (5), 1221.

Fiolleau, S., Uhlemann, S., Wielandt, S. and Dafflon B. 2023. Understanding slow-moving landslide triggering processes using low-cost passive seismic and inclinometer monitoring. *Journal of Applied Geophysics*, **215**, 105090.

Garin, H. (ed.), Baldwin, M., Reiffsteck, P., van der Made, K.-J., Wudtke, R., Lamas, L., Virely, D. and Polo Lopez, C.S. 2024. Assembling the Ground Model and the Derived Values. Guidelines for the Application of the 2nd Generation of Eurocode 7: Geotechnical Design. Publications Office of the European Union, Luxembourg, 156 pp.

Godlewski, T. and Szczepański, T. 2015. *Methods of soil stiffness determination in geotechnical investigations. Guidelines*. Warsaw: Building Research Institute (ITB). [in Polish]

Harba, P. and Pilecki, Z. 2017. Assessment of time–spatial changes of shear-wave velocities of flysch formation prone to mass movements by seismic interferometry with the use of ambient noise. *Landslides*, **14**: 1225–1233.

Harba, P., Pilecki, Z. and Krawiec K. 2019. Comparison of MASW and seismic interferometry with use of ambient noise for estimation of S-wave velocity field in landslide subsurface. *Acta Geophysica*, **67**: 1234–1247.

Hardin, B.O. and Drnevich, V.P. 1972. Shear modulus and damping in soils: Design equations and curves. *Journal of the Soil Mechanics and Foundations Division*, **98**, (SM7): 667–692.

Huntley, D., Bobrowsky, P., Hendry, M., Macciotta, R., Elwood, D., Sattler, K., Best, M., Chambers J. and Meldrum P., 2019. Application of multi-dimensional electrical resistivity tomography datasets to investigate a very slow-moving landslide near Ashcroft, British Columbia, Canada. *Landslides*, **16** (5), 1033–1042.

Institute of Geotechnics, Faculty of Environmental Engineering, Cracow University of Technology. 2010a. Geotechnical conditions for 17 monitored landslides based on laboratory tests (geotechnical analyses and direct shear tests), Mała landslide (near Dębica). Cracow University of Technology, Kraków. [in Polish]

Institute of Geotechnics, Faculty of Environmental Engineering, Cracow University of Technology, 2010b. Geotechnical conditions for 17 monitored landslides based on laboratory tests (geotechnical analyses and direct shear tests), Słotowa landslide. Cracow University of Technology, Kraków. [in Polish]

Intrieri, E., Frodella, W., Raspini, F., Bardi, F. and Tofani, V. 2020. Using satellite interferometry to infer landslide sliding surface depth and geometry. *Remote Sensing*, **12**, 1462.

Jaboyedoff, M., Oppikofer, T., Abellán, A., Derron, M.-H., Loye, A., Metzger, R. and Pedrazzini, A. 2012. Use of LiDAR in landslide investigations: A review. *Natural Hazards*, **61** (1), 1–25.

Jongmans, D., Fiolleau, S. and Bièvre, G. 2021. Geophysical monitoring of landslides: State-of-the-art and recent advances. In: Frodella, W., Moretti, S., Intrieri, E. (eds), *Natural Hazards: Monitoring, Prediction, and Mitigation*. Springer, Cham, pp. 177–212.

Kos J. 2021. Stability of landslide slopes based on physical and mechanical properties of rocks and soils and inclinometer measurements. *Biuletyn Państwowego Instytutu Geologicznego*, **478**, 15–48. [in Polish]

Luhn, J., Stumvoll-Schmaltz, M.J., Flores Orozco, A. and Glade, T. 2023. Internal structure of an active landslide based on ERT and DP data: New insights from the Hofermühle landslide observatory in Lower Austria. *Geomorphology*, **441**, 108910.

Mainsant, G., Larose, E., Brönnimann, C., Jongmans, D., Michoud, C. and Jaboyedoff, M. 2012. Ambient seismic noise monitoring of a clay landslide: Toward failure prediction. *Journal of Geophysical Research: Earth Surface*, **117**, F01030.

Marciniak, A., Kowalczyk, S., Oryński, S., Cader, J., Chambers, J., Stan-Kłeczek, I. and Majdański M. 2024. Four years of landslide observation with anthropogenic loading as an additional trigger: Analysis of seasonal and annual variability of physical parameters. *Engineering Geology*, **342**, 107761.

Merritt, A.J., Chambers, J.E., Wilkinson, P.B., West, L.J., Murphy, W., Gunn, D. and Uhlemann S. 2016. Measurement and modelling of moisture–electrical resistivity relationship of fine-grained unsaturated soils and electrical anisotropy. *Journal of Applied Geophysics*, **124**, 155–165.

Mugnai, F., Masiero, A., Angelini, R. and Cortesi, I. 2023. High-resolution monitoring of landslides with UAS photogrammetry and digital image correlation. European Journal of Remote Sensing, **56** (1), 2216361.

Nescieruk, P., Perski, Z., Wojciechowski, T., Warmuz, B., Kos, J., Curyło, J., Karwacki, K., Drożdżewski, M., Zając, M. and Dacka J. 2024a. *Monitoring report for the Mała landslide (No. 18-15-033 78473) under the project "System Osłony Przeciwosuwiskowej (SOPO), Stage III"*. Polish Geological Institute – National Research Institute, Kraków, 30 pp. [in Polish]

Nescieruk, P., Perski, Z., Wojciechowski, T., Warmuz, B., Kos, J., Curyło, J., Karwacki, K., Drożdżewski, M., Zając, M., and Dacka J. 2024b. *Monitoring report for the Słotowa landslide (No. 18-03-063 71897) under the project "System Osłony Przeciwosuwiskowej (SOPO), Stage III"*. Polish Geological Institute – National Research Institute, Kraków, 28 pp. [in Polish]

Nescieruk, P., Rączkowski, W., Wojciechowski, T., Warmuz, B., Michalski, A. and Dacka, J. 2014. *Geological documentation of monitoring works performed on the Słotowa landslide (SOPO, Stage II).* Polish Geological Institute – National Research Institute, Kraków, 31 pp. [in Polish]

Nescieruk, P., Wojciechowski, T., Warmuz, B., Karwacki, K., Kos, J., Curyło, J., Drożdżewski, M. and Dacka J. 2010. *Engineering-geological documentation for the Mała landslide (No. 18-15-033 78473) prepared within the project "System Osłony Przeciwosuwiskowej (SOPO), Stage I".* Polish Geological Institute – National Research Institute, Kraków, 45 pp. [in Polish].

Ostrowski, S., Rybak-Ostrowska, B. and Lasocki, M. 2013. Application of near-surface geophysical survey for recognition of the geology of landslide areas in the Carpathians: A case study. *Przegląd Geologiczny*, **61**, 67–73. [in Polish]

Ostrowski, S., Pacanowski, G., Majer, E., Sokołowska, M. (eds), 2023. *Badania geologiczno-inżynierskie. Geofizyka inżynierska.* Państwowy Instytut Geologiczny – Państwowy Instytut Badawczy, Warszawa, 329 pp. ISBN 978-83-67567-36-7. [in Polish]

Ouellet, S.M., Dettmer, J., Lato, M.J., Cole, S., Hutchinson, D.J., Karrenbach, M., Dashwood ,B., Chambers, J.E. and Crickmore R. 2024. Previously hidden landslide processes revealed using distributed acoustic sensing with nanostrain-rate sensitivity. *Nature Communications*, **15**, 6239.

Pazzi, V., Morelli, S. and Fanti, R. 2019. A review of the advantages and limitations of geophysical investigations in landslide studies. *International Journal of Geophysics*, 2019: 2983087.

Peduto, D., Santoro, M., Aceto, L., Borrelli, L. and Gullà, G. 2021. Full integration of geomorphological, geotechnical, A-DInSAR and damage data for detailed geometric-kinematic features of a slow-moving landslide in an urban area. *Landslides*, **18** (4), 807–825.

Perski, Z., Wojciechowski, T., Wójcik, A. and Borkowski, A. 2014. Monitoring of landslide dynamics with LiDAR, SAR interferometry and photogrammetry: Case study of the Kłodne landslide (Southern Poland). In: *Proceedings of the 3rd World Landslide Forum*, Beijing, 2–6 June 2014, 5 pp.

Polish Geological Institute – National Research Institute (PGI–NRI), 2016. Deep monitoring report: inclinometric measurements at the Mała landslide under the project "Monitoring of mass movement hazards together with maintenance of the existing observation network". Kraków, 20 pp [in Polish].

Rahimi, S., Wood, C.M. and Bernhardt-Barry, M. 2021. The MHVSR technique as a rapid, cost-effective and non-invasive method for landslide investigation: Case studies of Sand Gap and Ozark, Arkansas, USA. *Landslides*, **18**, 2039–2055.

Salciarini, D., Lupattelli, A., Cecinato, F., Cattoni, E. and Volpe E. 2022. Static and seismic numerical analysis of a shallow landslide located in a vulnerable area. *Rivista Italiana di Geotecnica*, **56** (2): 5–23.

Šegina, E., Peternel, T., Urbančič, T., Realini, E., Zupan, M., Jež, J., Caldera, S., Gatti, A., Tagliaferro, G., Consoli, A., Reyes González, J. and Jemec Auflič, M. 2020. Monitoring surface displacement of a deep-seated landslide by a low-cost and near real-time GNSS system. *Remote Sensing*, **12** (20): 3375.

Seitone, F., Vergnano, A., Comina, C., Bonasera, M. and Fubelli, G. 2025. Comparative analysis of geological and seismic microtremor models of a large translational landslide: The case of San Vito Romano, Central Italy. *Engineering Geology*, **347**, 107934.

Stark, M., Zieher, T., Rutzinger, M., Perzl, F. and Proske, H. 2020. The Salcher landslide observatory: Investigations on kinematics and structure of a complex landslide. *Bulletin of Engineering Geology and the Environment*, **79**, 1841–1857.

Uhlemann, S., Hagedorn, S., Dashwood, B., Maurer, H., Gunn, D., Dijkstra, T. and Chambers, J. 2016. Landslide characterization using P- and S-wave seismic refraction tomography: The importance of elastic moduli. *Journal of Applied Geophysics*, **134**, 64–76.

Uhlemann, S., Chambers, J., Wilkinson, P., Maurer, H., Merritt, A., Meldrum, P., Kuras, O., Gunn, D., Smith, A. and Dijkstra, T. 2017. Four-dimensional imaging of moisture dynamics during landslide reactivation. *Journal of Geophysical Research: Earth Surface*, **122**, 398–418.

Watlet, A., Wilkinson, P., Whiteley, J., White, A., Uhlemann, S., Swift, R., Ouellet, S., Minto, C., Meldrum, P., Jones, L., Gunn, D., Godfrey, A., Dashwood, B., Crickmore, R., Clarkson, P., Boyd, J. and Chambers J. 2024. High-resolution geophysical monitoring of moisture accumulation preceding slope movement: A path to improved early warning. *Environmental Research Letters*, **19** (12), 124059.

Warmuz, B. and Nescieruk, P. 2019. Dynamika przemieszczeń wybranych osuwisk w Karpatach (The dynamics of displacements of selected landslides in the Carpathians). *Przegląd Geologiczny*, **67**, 326–331.

Whiteley, J.S., Chambers, J.E., Uhlemann, S., Wilkinson, P.B. and Kendall, J.M. 2019. Geophysical monitoring of moisture-induced landslides: A review. *Reviews of Geophysics*, **57**, 106–145.

Whiteley, J.S., Chambers, J.E., Uhlemann, S., Boyd, J., Cimpoiașu, M.O., Holmes, J.L., Inauen, C.M., Watlet, A., Hawley-Sibbett, L.R., Sujitapan, C., Swift, R.T. and Kendall, J.M. 2020. Landslide monitoring using seismic refraction tomography: The importance of incorporating topographic variations. *Engineering Geology*, **274**, 105525.

Manuscript submitted: 12th December 2025
Revised version accepted: 3rd June 2026